

A high-throughput exploration of magnetic materials by using structure predicting methods

S. Arapan, P. Nieves, and S. Cuesta-López

Citation: *Journal of Applied Physics* **123**, 083904 (2018); doi: 10.1063/1.5004979

View online: <https://doi.org/10.1063/1.5004979>

View Table of Contents: <http://aip.scitation.org/toc/jap/123/8>

Published by the *American Institute of Physics*

Articles you may be interested in

[Engineering electric and magnetic dipole coupling in arrays of dielectric nanoparticles](#)

Journal of Applied Physics **123**, 083101 (2018); 10.1063/1.5018312

[Simulation study of ballistic spin-MOSFET devices with ferromagnetic channels based on some Heusler and oxide compounds](#)

Journal of Applied Physics **123**, 084503 (2018); 10.1063/1.5011328

[Mediating exchange bias by Verwey transition in CoO/Fe₃O₄ thin film](#)

Journal of Applied Physics **123**, 083903 (2018); 10.1063/1.5023725

[Relativistic quasiparticle band structures of Mg₂Si, Mg₂Ge, and Mg₂Sn: Consistent parameterization and prediction of Seebeck coefficients](#)

Journal of Applied Physics **123**, 085114 (2018); 10.1063/1.5018186

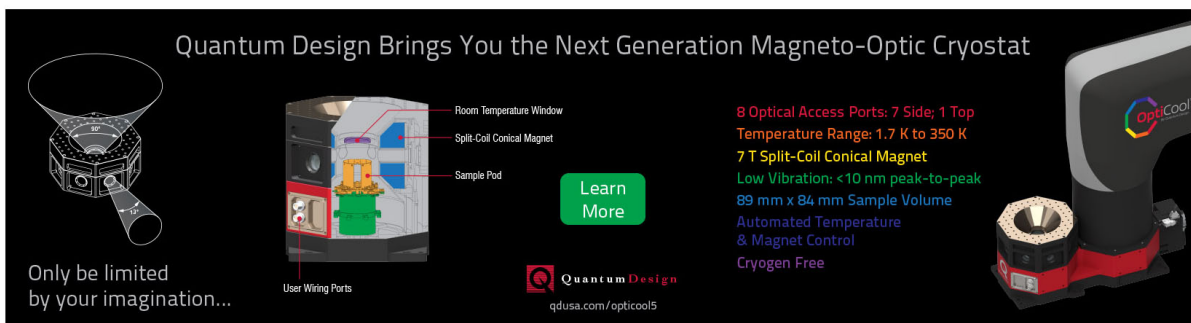
[Characterization of individual layers in a bilayer electron system produced in a wide quantum well](#)

Journal of Applied Physics **123**, 084301 (2018); 10.1063/1.5019655

[Raman effect in multiferroic Bi₅Fe_{1+x}Ti_{3-x}O₁₅ solid solutions: A temperature study](#)

Journal of Applied Physics **123**, 084101 (2018); 10.1063/1.5019291

Quantum Design Brings You the Next Generation Magneto-Optic Cryostat



Only be limited by your imagination...

Learn More

Quantum Design
qdusa.com/opticool5

8 Optical Access Ports: 7 Side; 1 Top
Temperature Range: 1.7 K to 350 K
7 T Split-Coil Conical Magnet
Low Vibration: <10 nm peak-to-peak
89 mm x 84 mm Sample Volume
Automated Temperature & Magnet Control
Cryogen Free

A high-throughput exploration of magnetic materials by using structure predicting methods

S. Arapan,^{1,2,a)} P. Nieves,^{1,2} and S. Cuesta-López^{1,2}

¹ICCRAM, International Research Center in Critical Raw Materials and Advanced Industrial Technologies, University of Burgos, 09001 Burgos, Spain

²Advanced Materials, Nuclear Technology and NanoBioTechnology Department, University of Burgos, 09001 Burgos, Spain

(Received 15 September 2017; accepted 9 February 2018; published online 28 February 2018)

We study the capability of a structure predicting method based on genetic/evolutionary algorithm for a high-throughput exploration of magnetic materials. We use the USPEX and VASP codes to predict stable and generate low-energy meta-stable structures for a set of representative magnetic structures comprising intermetallic alloys, oxides, interstitial compounds, and systems containing rare-earths elements, and for both types of ferromagnetic and antiferromagnetic ordering. We have modified the interface between USPEX and VASP codes to improve the performance of structural optimization as well as to perform calculations in a high-throughput manner. We show that exploring the structure phase space with a structure predicting technique reveals large sets of low-energy metastable structures, which not only improve currently existing databases, but also may provide understanding and solutions to stabilize and synthesize magnetic materials suitable for permanent magnet applications. © 2018 Author(s). All article content, except where otherwise noted, is licensed under a Creative Commons Attribution (CC BY) license (<http://creativecommons.org/licenses/by/4.0/>). <https://doi.org/10.1063/1.5004979>

I. INTRODUCTION

Advances in computer technology and continuous development of numerical methods have revolutionized the way of performing research within materials science. Nowadays, one can setup a virtual lab and “synthesize” new materials with just the help of a computer. Several important factors had contributed to such an evolution. A new way to do research of material properties was opened by successful implementation of Density Functional Theory (DFT) methods¹ for the prediction of the electronic structure of materials and, hence, their physical properties from first principles at relatively modest computational costs. Further advance has been made by development of efficient statistical methods for analyzing the huge amount of experimental and theoretical data in order to elucidate correlations between different properties of materials: structural, physical, chemical, etc. With the knowledge of such correlations, both experimentalists and computational physicists could predict and synthesize new materials with desired properties: the former in a lab, combining chemistry with physical methods, and second on a computer by performing *ab-initio* calculations. With the help of high-throughput computational methods, large databases have been created,^{2,3} which provide structural and thermodynamic data for a large amount of known compounds as well as many hypothetical structures.

Yet, until recently, computational methods were still inferior to experimental ones when it comes to predicting a structure and its properties from scratch. In order to predict or describe the properties of a material numerically, one needs as an input its structural information. This disadvantage,

however, may become part of the past with the introduction of structure predicting techniques based on evolutionary or adaptive genetic algorithms (AGA). Linked with *ab-initio* methods, AGA based structure prediction opens a promising prospect for discovering new materials with given properties. And at the same time, this method will complement the data analysis technique.

We are experiencing an increasing influence of modern technology on our daily life, thus continuous technological improvement is in the focus of the material science community. Magnetic materials play an important part in modern technology (data processing, energy conversion), and performant magnets are in great demand. The performance of a permanent magnet, however, depends on the amount of critical raw materials (mainly rare-earth) present in its composition. A considerable amount of attention is paid now to manufacturing competitive rare-earth free permanent magnets. It is needless to say that this problem presents also a challenge from the fundamental point of view of understanding the interplay of structural parameters and physical properties of constituting elements in formation of a permanent magnet. We have recently proposed to tackle this problem via computational methods by using AGA for structure predicting,⁴ and in our investigation we chose the code USPEX.⁵ It became popular recently within the materials science community, by predicting new phases under pressure for materials relevant for the interior of Earth, as well as other remarkable high-pressure phases.^{6–8}

The efficiency of exploring a large number of structures with structure predicting methods depends strongly on the performance of the structural optimization. Computationally, magnetic materials add an extra degree of complexity due to

^{a)}Electronic mail: sergiu.arapan@gmail.com

magnetic interaction. First, there exists a different magnetic order. Second, an accurate account for localized magnetic moment requires going beyond standard DFT calculations. The *ab-initio* code VASP⁹ is a versatile tool to perform accurate structural optimization, and the USPEX code is interfaced with VASP, providing a way to relax structures generated by USPEX. In the current study, we have designed our own scheme for VASP calculations, with details given in Sec. II. First, we study the efficiency of our scheme of predicting stable structures for various representative magnetic materials. Second, we explore the space of low-energy metastable phases of these magnetic compounds. Results of this investigation are provided in Sec. III, and are complemented with discussion of various mechanisms that produced a structure during the evolutionary search, and the analysis of low-energy metastable structures and comparison with available databases. This paper finally concludes with the summing-up in Sec. IV.

II. METHODS

USPEX uses an evolutionary algorithm to generate different structures. It uses as an input the number and type of ions to be considered within the unit cell only. At the first step, a set of structures is generated at random, by randomly choosing a crystal space group, corresponding lattice vectors, and ion positions. Structures generated in such a way, are, obviously, far from their equilibrium. Thus, performing a structure relaxation is required to estimate accurately the energy of a structure, which serves as a fitness criterion. A subset of fitted structures is selected to generate a next generation of structures by means of genetic operations (crossover and mutations). The process of random generations of structures is performed also at each step to provide a diversity of structures for each generation. The search for an optimal structure is performed until no new best structures are generated for a certain number of generations or the maximum number of generations is reached. We have also performed calculations with several formula units for each compound.

USPEX is interfaced with several numerical codes, based on *ab-initio* or classical molecular dynamics methods, able to perform structural relaxation. Among them, VASP is, currently, one of the most reliable codes in terms of accuracy and versatility.¹⁰ All VASP calculations were performed with the PAW PBE 5.4 potentials,^{11,12} with an energy cut-off up to 1.4 of the default VASP energy cut-off, and an automatic *k-points* generating scheme with a scaling factor starting from 10 to 30. In the current study, the way the VASP performs the structural optimization is controlled by an auxiliary script, which allows for greater flexibility for running calculations than the original USPEX setup. The purpose is twofold: (i) improving the performance of structural optimization (better accuracy of calculations and shorter calculation times), and (ii) performing the calculations in an adaptive and automated way. We follow the same prescription of performing structural optimization in several steps, increasing the accuracy at each step. But we have introduced several modifications, which makes the search for magnetic structures more efficient. First, it is starting with non-spin-polarized calculation at a larger volume, performing shape and ion position relaxations. Second, it is switching to the

spin-polarized calculations and adding volume relaxation with an increased energy cut-off. Finally, it is getting the equilibrium parameters via a series of shape and ion position optimizations at given volumes by fitting $E = E(V)$ to an equation of state (EOS). A check of the job status is performed at each relaxation step. In the case of an error, calculations are restarted with relevant parameters changed on the fly. At each stage, a refinement of the symmetry of the relaxed structure is performed. At the end of structural relaxation, an additional calculation is performed with a different magnetic order and the lowest energy is considered (in this study we consider only collinear spin configurations). We have performed few runs by calling the VASP program through the standard USPEX scheme and by our script and the comparison shows a speed-up of calculations up to 30% (for a structure with 6 atoms).

For our study, we have chosen some representative magnetic materials¹³ as well as some magnetic compounds of interest to the development of rare-earth free permanent magnets. We tried to study across different types of magnetic materials, like metallic alloys, oxides, and system with localized magnetic moments, featuring both ferromagnetic and antiferromagnetic ordering. Crystal structures of considered systems are shown for convenience in Fig. 1. We have tried to be as unbiased as possible, taking as an input the unit formula of the compound and its magnetic ordering as additional information. For each compound, we started by performing a search with one formula unit, then increasing the number of atoms to two formula units, and, providing that the number of ions in the unit cell is less than 10–15, increasing further up to three formula units. Although using DFT calculations yields accurate results, the cubic scaling of the computational effort with the number of ions in the unit cell imposes a hard limit on the size of investigated system. In addition, the size of the population scales in a linear fashion with the number of ions, since the number of structures considered within one generation in USPEX is a factor of two or three larger than the number of ions. In almost all of the USPEX calculations, we used the following settings for producing the next generation. A fraction of 0.65 of best structures of current generation have been chosen to evolve to the next one. 40% of structures were produced by heredity, 10% by permutations, and another 10% by soft-mutations. The remaining 40% of structures were generated at random. The maximum number of generations was set to 30 and the convergence criterion set to 15 generations. All USPEX calculations ended by reaching the convergence criterion. After completion of a set of calculations with one, two and/or three formula units we have analyzed the results and compared against reference data.

III. RESULTS AND DISCUSSION

In the following, we will present in some detail the obtained results. We began our exploration by considering intermetallic magnetic compounds, which form into the ordered L1₀ structure and are the focus of the current efforts for making a permanent magnet from some magnetic materials adopting this structure. A representative compound is the CoPt.¹³ The L1₀ phase forms around the equiatomic

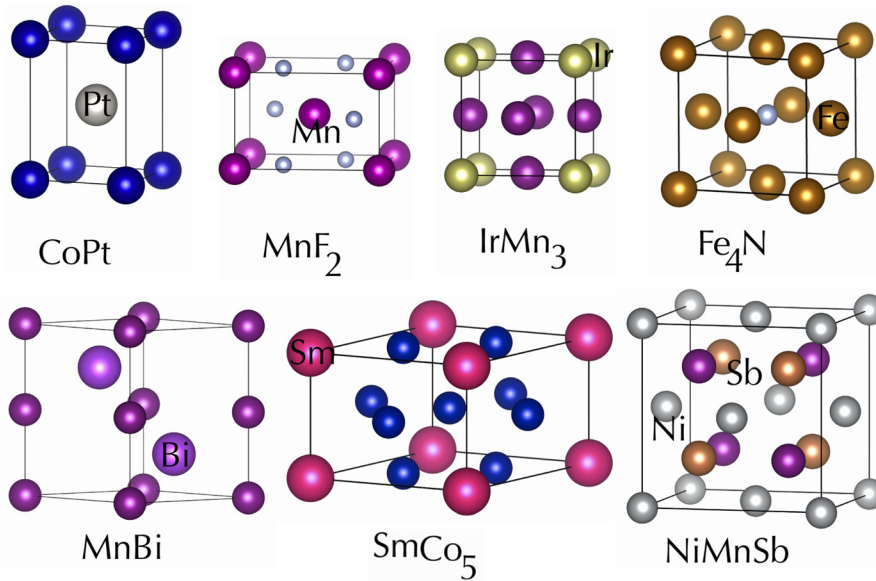


FIG. 1. Crystal structures of some representative magnetic materials used for the high-throughput exploration by using structure prediction.

composition (25% to 60% Co) of CoPt alloys at elevated temperature from the disordered A1 structure.¹⁴ The L1₀ CoPt is a good performance permanent magnet, which exhibits high Curie temperature ($T_C = 840$ K), high saturation magnetization ($\mu_0 M_S = 1$ T), and very high uniaxial anisotropy ($K_u = 4.9$ MJ/m³).¹³ It is used in medical and military applications, as well as in precision instrument manufacturing, but is costly because of Co and Pt high supply risk.¹⁵

We performed several runs for structures with one, two, and three formula units in the unit cell. In all cases, the L1₀ structure was found as the stable structure. For the run with one formula unit, the size of population of one generation was 6 structures. The stable CoPt structure was obtained in the second generation by heredity from a structure with cubic symmetry, the B2 structure, space group #221, and another one with hexagonal symmetry, space group #191, which were the best structures of the first generation. About 90 structures were generated, but all of them relaxed to just

8 distinct symmetry groups. Calculations were run in parallel with 2 cores/job and finished in about 6 h. For the run with two formula units in the unit cell, the size of the population was 10 structures, and the L1₀ structure was obtained at the start by random generation. About 150 structures were generated, which relaxed in structures with 20 distinct symmetry groups. Jobs were run in parallel with 2 cores/job and took about 36 h. Finally, in the run with three formula units per unit cell the L1₀ structure was obtained in the second generation by soft-mutation from a structure with the hexagonal symmetry, space group #164, which was the best among first generation. Soft-mutations are structural changes induced by displacing atoms along the softest mode eigenvector or a random linear combination of soft mode vectors. About 250 structures were calculated with 31 distinct symmetries and calculations ran for about 180 h. An intuitive graphical representation of the described process of getting the L1₀ structure of CoPt by means of genetic operations is shown in Fig. 2.

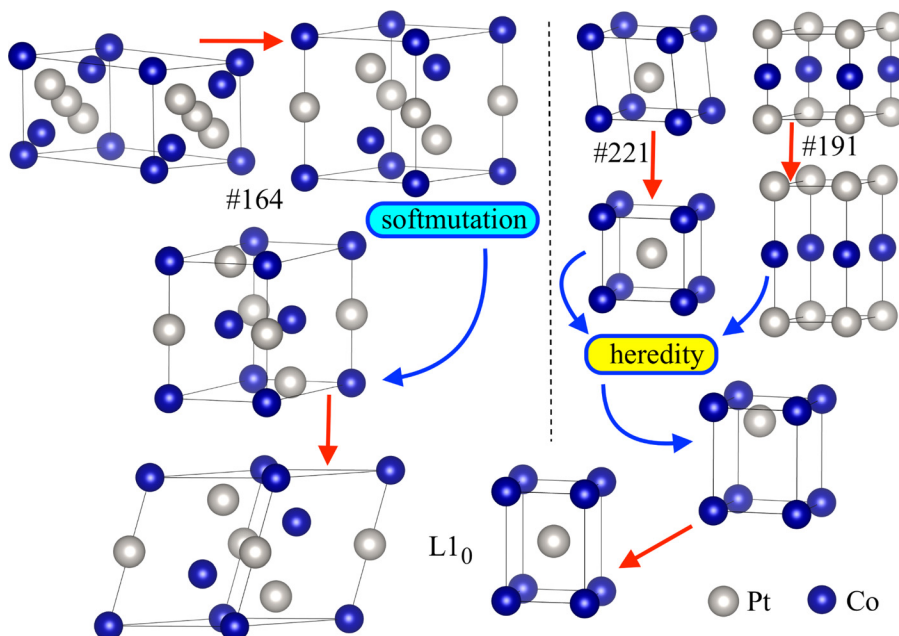


FIG. 2. The process of predicting the L1₀ phase of CoPt by using the genetic algorithm implemented in USPEX for a structure with one formula unit per unit cell (right) and three formula units per unit cell (left). In the case of one formula unit, the first row of structures (from top to bottom) is structures generated randomly in the first generations. In the second row, relaxed structures are shown (the relaxation process is schematically represented by red arrows and labels provide the space group number). In the second generations (third row), structures are obtained via genetic operations: a crossover of two structures (heredity). The structure finally relaxes towards the L1₀ structure. In the case of three formula units, the genetic operation, which leads to the L1₀ structure, is a softmutation of a relaxed structure.

We applied a similar procedure for two other compounds, which adopt the $L1_0$ structure: MnAl and FeNi. The $L1_0$ FeNi alloy has attracted a great deal of attention because it has a large uniaxial magnetic anisotropy energy (MAE) with $K_u = 1.3 \text{ MJ/m}^3$, and nearly the same saturation magnetization, $\mu_0 M_s = 1.59 \text{ T}$, as $\text{Nd}_2\text{Fe}_{14}\text{B}$, with high Curie temperature and corrosion resistance.¹⁶ Unfortunately, the formation of the $L1_0$ phase in FeNi is extremely sluggish. So far, the only bulk FeNi sample in the $L1_0$ phase was found in meteorites, where it took billions of years to be transformed under extreme conditions and temperatures.¹⁷ In MnAl, the $L1_0$ (τ -phase) forms in metastable ferromagnetic MnAl compound in a range of compositions stretching from 51% to 58% Mn.^{18,19} In experiments, the A3 antiferromagnetic ϵ -phase transforms to an intermediate orthorhombic ferromagnetic ϵ' -phase at high temperatures, which leads to the metastable ferromagnetic τ -phase.²⁰ The MnAl τ -phase is a promising permanent magnet, which exhibits high Curie temperature ($T_C = 650 \text{ K}$), high saturation magnetization ($\mu_0 M_s = 0.75 \text{ T}$), high uniaxial anisotropy ($K_u = 1.7 \text{ MJ/m}^3$), and very low cost.²¹ However, its metastable nature and moderate coercivity ($H_C = 0.2 - 0.8 \text{ MA/m}$)²² prevent it from being manufactured for permanent magnet applications.

For both compounds, we performed runs with a number of atoms per unit cell from one to four formula units and all runs predicted the $L1_0$ phase as the stable one. As in the case of CoPt, the $L1_0$ structure is obtained by various genetic operations. For the MnAl, for example, the $L1_0$ structure emerged as result of crossover in the second generation for one and three formula unit runs, and was randomly generated in the second generation for the two formula unit run and in the fourth generation for the four formula units run. In the case of FeNi, the $L1_0$ structure was obtained by heredity in the second generation for the one formula unit and two formula unit runs, in the seventh generation for the three formula unit run, and randomly generated in the first generation for the four formula unit run.

Although the $L1_0$ is a simple basic structure and could be predicted by just performing a random search, the evolutionary algorithm implemented in the USPEX code allows us to get this structure easy as a result of genetic operations. In Fig. 3, we show the energy distribution of generated structures during 16 generation for the case of CoPt with a three formula unit run. We can see that randomly generated structures, represented by red disks, span a large energy interval [Fig. 3(a)] and most of them are energetically very unstable, while most of the relevant metastable phases are generated as a result of various genetic operations. If we consider that an energy window of $\Delta E = 200 \text{ meV}$ above the ground state, E_0 , contains most of the relevant metastable phases, then we could roughly estimate the performance of random structure sampling compared to that of the genetic algorithm method as the ratio of number of randomly generated structures with energy $E_0 < E < E_0 + \Delta E$, and all generated structures within the same energy window [Fig. 3(b)]. It is obvious that this ratio will be determined by the number of atoms in the unit cell, decreasing with increasing the number of atoms. In the case of one formula unit run (2 atoms) for all compounds that adopt the $L1_0$ structure, this ratio is about 0.2, while for

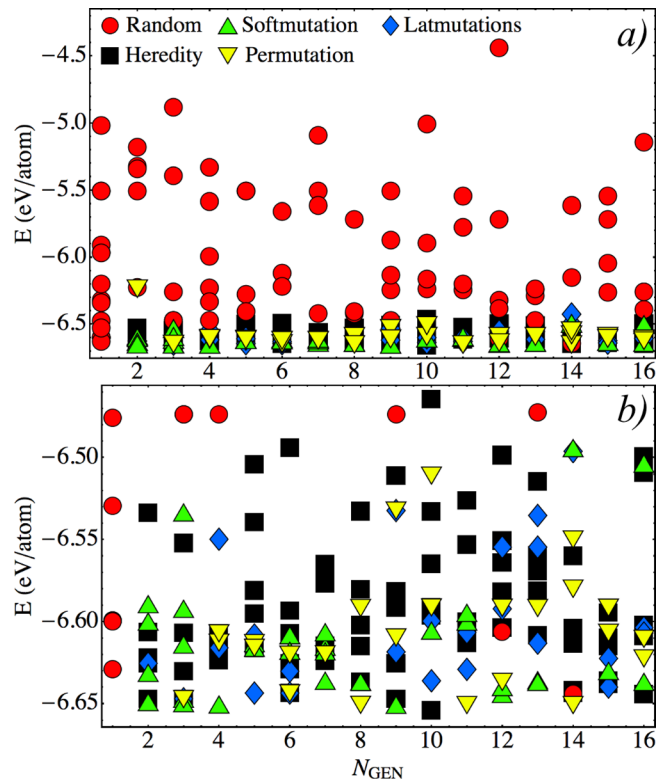


FIG. 3. Energy distribution of structures generated during 16 generations for the case of CoPt with the three formula unit run: (a) all generated structures, and (b) structures within 200 meV interval above the ground state. Different symbols show the origin of generated structures: random generation (red disks) or as a result of certain genetic operation.

the three formula unit run (6 atoms) the ratio is about 0.1. These results are consistent with other tests,²³ which clearly shows that the evolutionary method outperforms the random sampling runs.

While predicting already known structures is more of a methodological interest, it is instructive to analyze the set of low-energy metastable structures generated by USPEX and see how this method of exploring the structural phase space compares with other high-throughput numerical techniques. We have selected metastable structures with energies less than 100 meV/atom above the stable phase. The results obtained for all three compounds are shown in Table I. We observe that these three different compounds have also similar metastable phases, but differently ordered energetically. Some structures differ, but tend to adopt similar symmetries. A remarkable fact is that the output of predicted phases is noticeably larger than the current available information from databases.

This extra information may help to understand why, for example, the disorder-order transition to the $L1_0$ phase in the FeNi is extremely slow. If we compare the energies of metastable phases in CoPt and FeNi, we can see that in the former compound exists a set of metastable structures very close (less than 20 meV/atom) in energy to the ground state, while in the FeNi the gap between the ground state structure and metastable phases is relatively large. We may speculate that these energetically low lying phases could facilitate the transition to the $L1_0$ structure in CoPt. We show crystal lattices of best predicted structures in CoPt in Fig. 4. We observe

TABLE I. Space group (#N) and energy/atom in meV (ΔE) above the ground state $L1_0$ phase for a set of metastable structures predicted by USPEX for CoPt, FeNi, and MnAl. We have bold faced structures that are present in the AFLOW library.²⁴ Indices discriminate structures with different Wyckoff positions of ions for the same symmetry.

CoPt		FeNi		MnAl	
Sym	ΔE	Sym	ΔE	Sym	ΔE
#65	3	#65 _b	26	#51	36
#51	4	#99	30	#123	41
#38	4	#38	31	#221	41
#8	9	#51	35	#65_b	50
#12	10	#11	35	#141	65
#123 _b	11	#123 _b	36	#129	66
#65 _b	14	#8	39	#12 _c	71
#99	20	#25	44	#8	77
#25	24	#12 _b	46		
#63	27	#129	47		
#5	28	#141	51		
#141	33	#59	52		
#10	34	#166	67		
#59	37	#187	69		
#187	53	#160	69		
#166	56				

three groups of structures within the best metastable phases. The first two best metastable structures with space group numbers #65 and #51 are orthorhombic distortions of the $L1_0$ phase. The structure #51 is present in the AFLOW database as the best metastable phase for the MnAl and could be the intermediate orthorhombic ferromagnetic ϵ' -phase.²⁰ A second set of structures shown in Fig. 4 (#38, #123_b, #65_b, #99) has as the basic element the orthorhombically distorted $L1_0$ cell with some swapped positions of Co and Pt atoms. This set of structures represents the group of best metastable phases for the FeNi, and the structure denoted as #65_b is also present in the AFLOW database for the MnAl. A third group comprises some low symmetry structures (#8 and #12), which seem to combine elements from the first two

mentioned groups. Finally, we can also see the presence of two low-energy metastable structures in MnAl, which represent the case of the $L1_0$ structures with $c/a < 1$, the #123 phase, and with $c/a = 1$, the #221 phase. Although these two phases can be obtained by small tetragonal distortions from the $L1_0$ phase, they are energetically very unstable (well above 100 meV/atom from the ground state) in CoPt and FeNi systems.

We have continued our study by considering few Mn-based magnetic compounds, like (i) MnBi, a representative material of ferromagnetic manganese pnictides, (ii) NiMnSb, representing the family of Heusler and half-Heusler alloys, (iii) IrMn₃ as an example of antiferromagnetic Mn-based alloys, and (iv) MnF₂, illustrating the antiferromagnetic fluorides.¹³ For all these examples, we performed calculations with one and two formula units per unit cell only, which has proven to be enough to predict the experimentally known structures.

MnBi is a hard ferromagnet with anisotropic magnetostriction. It exhibits good magneto-optic properties due to the strong spin-orbit coupling of Bi. The B8₁ hexagonal structure of MnBi was randomly generated at the 8th generation during the run with two formula units. Structures generated during the one formula unit run were all energetically very unfavorable separated by a gap larger than 100 meV/atom above the ground state. We have found 4 structures of MnBi with one formula unit present in the AFLOW and all of them were generated during the USPEX run. For structures with two formula units, AFLOW provides one metastable structure, which also is reproduced by our search. A list of metastable structures is shown in Table II.

NiMnSb was one of the first materials to be identified as a half-metal and is an example of a half-Heusler XYZ alloy, with ions X, Y, and Z arranged on four interpenetrating A1 lattices. It is also the only ternary compound we have tried to predict with USPEX. The experimentally known structure, the C1_b phase, was predicted for both, one formula unit and two formula units, runs. There are six C1_b structures of

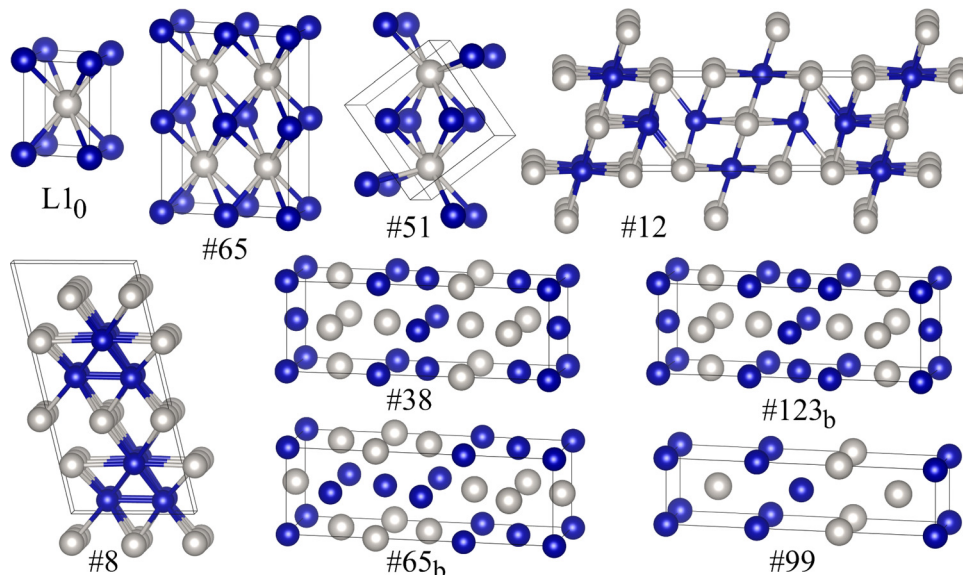


FIG. 4. Crystal lattices of best predicted structures for CoPt.

TABLE II. Space group (#N) and energy/atom in meV (ΔE) above the corresponding ground state phase for a set of metastable structures predicted by USPEX for MnBi, NiMnSb, and IrMn₃. We have bold faced structures that are present in the AFLOW²⁴ or Materials Project libraries. Indices discriminate structures with different Wyckoff positions of ions for the same symmetry.

BiMn		NiMnSb		IrMn ₃	
Sym	ΔE	Sym	ΔE	Sym	ΔE
#129	40	#166	72	#71	13
#166 _b	67	#127	18
...	...	#216_b	323	#12	23
#225	133		
#166	133			#194	42
#65	196			#59	60
#187	230			#25	86

NiMnSb available in the AFLOW database corresponding to different arrangements of Ni, Mn, and Sb ions on the A1 lattices. All of these structures are found during the evolutionary search. In fact, all possible permutations of ions lead to two distinct structures only: the ground state one and a very unstable one (denoted **#216_b** in Table II). For the one formula unit run, the unstable structure was obtained in the first generation, while the stable structure was obtained in the second generation in two ways: as a crossover between two low symmetry structures and a soft-mutation of another low symmetry structure. In the two formula unit run, the C1_b phase was obtained in the 8th generations by heredity. We have obtained only one metastable structure with energy less than 100 meV/atom above the ground state during the two formula unit run.

The MnF₂ is a model antiferromagnet, which adopts the tetragonal rutile (C4, space group #136) structure.¹³ Magnetic moments are collinear and we have predicted this structure in a two formula unit run. We ran several calculations with different magnetic orders, and the rutile phase with the antiferromagnetic arrangement of magnetic moments emerged as the stable one in all runs. In one run, the rutile structure was randomly generated, while in another run it evolved through a series of genetic operations. First, a tetragonal anatase structure (C4, space group #141), best in the first generation, underwent a softmutation in the second generation, and the resulting structure a lattice mutation to yield the rutile structure in the third generation. Interestingly, the initial anatase structure is the lowest metastable structure (25 meV/atom above the ground state) found during the two formula unit run. We have found two metastable structures in the Materials Project database, but with three formula units per unit cell: one (space group #60) just 2 meV/atom above the rutile structure, and the second (space group #68) at 48 meV/atom above the stable phase. Similar to MnF₂, the only binary oxide that is ferromagnetic metal, CrO₂, also forms in the rutile structure.¹³ USPEX revealed the rutile structure to be the stable one for CrO₂ during the two formula units run, as well as the anatase phase to be the best metastable structure at 53 meV/atom above the ground state structure. Two metastable phases, which are present in the Materials Project database, correspond to four and eight formula units

structures and energetically are close to the C5 structure (about 50 meV/atoms above the ground state).

An interesting case is the IrMn₃ compound. It is an antiferromagnet frequently used for exchange bias in thin-film devices.¹³ It adopts the cubic L1₂ structure and has a non-collinear arrangement of magnetic moments. In principle, we cannot predict the ground state structure by performing standard collinear spin-polarized DFT calculation. A collinear arrangement of Mn magnetic moments results in a ferrimagnetic state with a slight tetragonal distortion of the L1₂ phase towards the L1₀ structure (Fig. 5). This structure was found during USPEX runs with different numbers of formula units. In fact, since the symmetry of a structure is determined with a low precision (in order to get as higher symmetry as possible), the stable structure yielded by USPEX was the L1₂ phase. There are several metastable structures with one and two formula units of IrMn₃ available in the AFLOW database, which are also predicted by USPEX. In addition, we have predicted a set of metastable states with much lower energies. Results are shown in Table II and Fig. 5, by considering the L1₀ structure as the ground state.

Best performance permanent magnets contain rare-earth elements like Nd, Dy, and Sm. Apart from searching for new rare-earth free permanent magnets, an intermediate solution would be finding stable magnetic phases with a lower content of rare-earth elements. For this reason, we included in our study an example of a rare-earth based ferromagnet. We have chosen the SmCo₅, the first rare-earth permanent magnet with the greatest anisotropy ($K_u = 17.2 \text{ MJ/m}^3$) and high Curie temperature ($T_C = 1020 \text{ K}$).¹³ It forms in the CaCu₅ (D2_d) hexagonal structure. The rare-earth elements have localized magnetic moments and, generally, require the use of DFT + U approach or use of hybrid energy functionals to describe the charge localization of the valence *f*-electrons. However, one may devise potentials, which “force” the charge localization in the core states and perform the standard DFT calculations. We have done only one formula unit run and the D2_d structure was predicted as the stable one several times by random generation. As the best metastable structure (about 100 meV above the ground state), we got a similar D2_d structure, but with a larger *c/a*-ratio and the Co atoms well separated by Sm planes (Fig. 5).

A set of interesting metastable phases emerged during the study of an example of interstitial magnetic compound, namely, the Fe₄N. The N stabilizes the A1 γ -Fe by occupying the body centre of the cubic cell.¹³ We performed several runs with one formula unit per unit cell, as well as a run with two formula units. We have obtained the experimentally known structure (space group #221) during the one formula unit run. This structure was predicted by different genetic operations: through softmutation in the second generation from a body-centered tetragonal structure (space group #139), and through heredity in the fifth generation with the same tetragonal structure as a parent. This tetragonal phase is the best metastable phase for the one formula run, higher by 12 meV/atom in energy than the ground state. The two formula unit run revealed a set of metastable structures very close in energy, with a

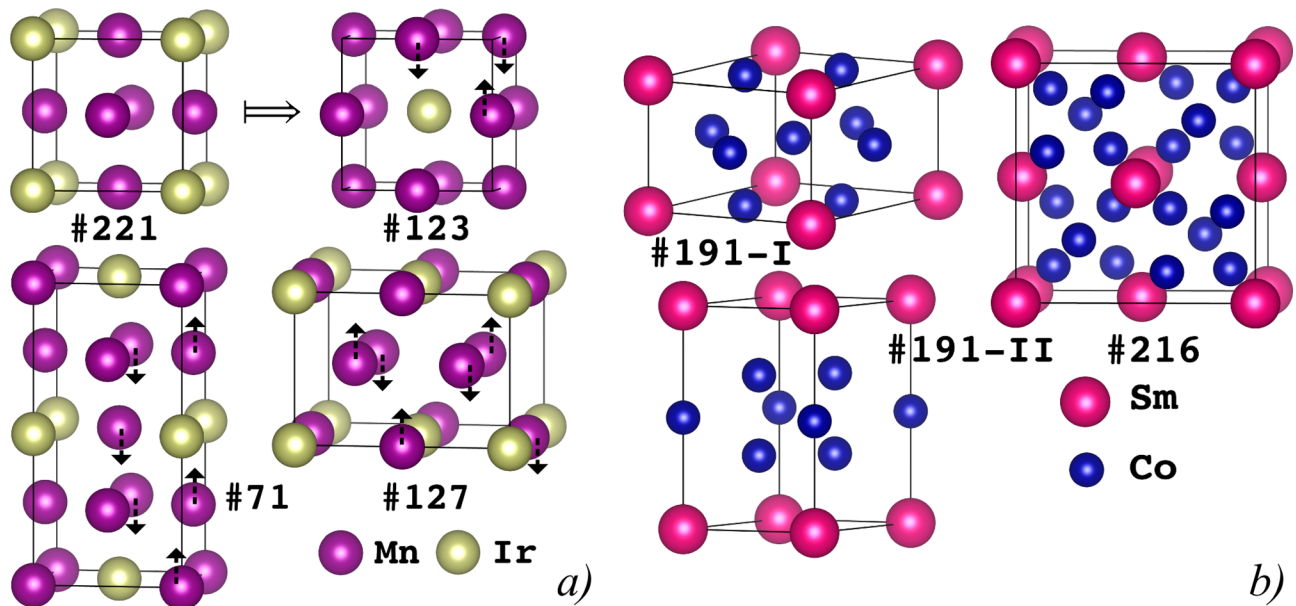


FIG. 5. Crystal structures of best energy states for (a) the MnIr_3 , and (b) the SmCo_5 compounds.

face-centered orthorhombic structure (space group #43) having virtually the same energy as the experimentally known structure and that could be stabilized under slight pressure. This set of metastable structures is shown in Fig. 6. In addition to the lattice structures, the difference in enthalpy with respect to the ground state phase of the Fe_4N as a function of pressure is shown to demonstrate the stabilization of these metastable structures with pressure.

IV. CONCLUSION

In this work, we have studied the efficiency of structure predicting methods based on evolutionary algorithms to massively explore the structural phase space of magnetic materials. In particular, we have modified the interface between VASP and USPEX codes to achieve an improved performance for structural optimization and run the calculations in

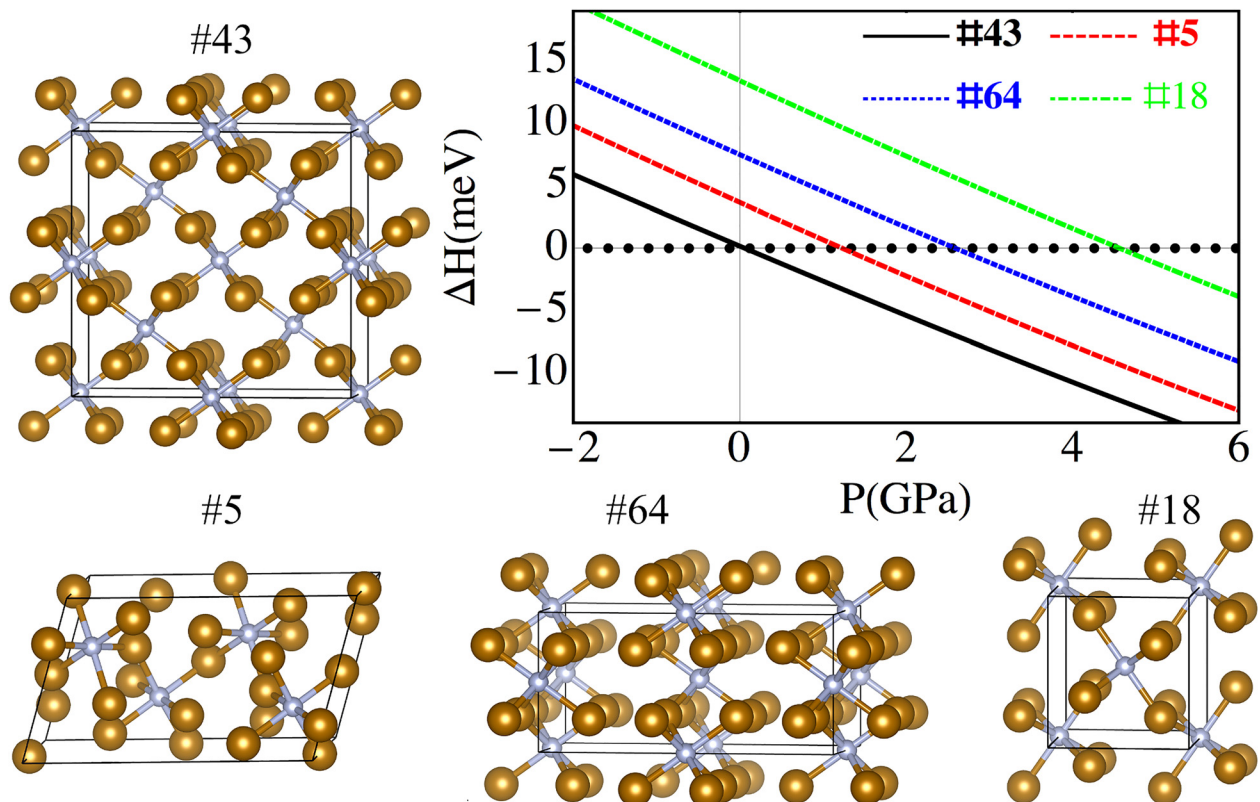


FIG. 6. Crystal lattices of best metastable structures predicted for Fe_4N and the variation of their enthalpies (with respect to the Fe_4N ground state structure) with pressure.

an adaptive and automated way. The evolutionary method implemented in the USPEX code provided a 100% success rate for the chosen set of magnetic structures (Fig. 1). Most importantly, the evolutionary search provides us with large sets of metastable phases, which not only complement existing structure databases, but go beyond the current high-throughput numerical methods. In this study, we show the richness of new metastable phases for magnetic compounds with the $L1_0$ ground-state phase, as well as interstitially stabilized magnetic compound Fe_4N . These metastable phases could provide us with a source of new magnetic structures with desirable properties, in particular, materials suitable for permanent magnet applications. Thus, the structure predicting methodology, based on genetic/evolutionary algorithms, is a powerful tool to improve our knowledge in a systematic way and provide valuable information for the Materials Genome project and for theoretical scientists and experimentalists designing novel functional materials.

ACKNOWLEDGMENTS

The authors would like to acknowledge funding support from the EU H2020 Program Project NOVAMAG: Novel, critical materials free, high anisotropy phases for permanent magnets, by design (Project ID: 686056). They would also like to thank the Spanish Supercomputing Network (RES) for granting computational resources on Magerit at CeSViMa, application QSM-2016-2-0034.

¹K. Lejaeghere *et al.*, *Science* **351**, aad3000 (2016).

²See <http://afloplib.org/> for information about structural and calculated physical properties of various crystal structures.

³See <https://materialsproject.org/> for information about structural and calculated physical properties of various structures.

⁴P. Nieves, S. Arapan, G. C. Hadjipanayis, D. Niarchos, J. M. Barandiaran, and S. Cuesta-López, *Phys. Status Solidi C* **13**, 942 (2016).

⁵See <http://uspeex.stonybrook.edu/uspeex.html> for information about USPEX code.

⁶A. R. Oganov and C. W. Glass, *J. Chem. Phys.* **124**, 244704 (2006).

⁷A. R. Oganov, A. O. Lyakhov, and M. Valle, *Acc. Chem. Res.* **44**, 227 (2011).

⁸A. O. Lyakhov, A. R. Oganov, H. T. Stokes, and Q. Zhu, *Comput. Phys. Commun.* **184**, 1172 (2013).

⁹See <https://www.vasp.at> for information about VASP code.

¹⁰G. Kresse and J. Furthmüller, *Phys. Rev. B* **54**, 11169 (1996).

¹¹G. Kresse and D. Joubert, *Phys. Rev. B* **59**, 1758 (1999).

¹²J. P. Perdew, K. Burke, and M. Ernzerhof, *Phys. Rev. Lett.* **77**, 3865 (1996).

¹³J. M. D. Coey, *Magnetism and Magnetic Materials* (Cambridge University Press, New York, 2010), Ch. 11.

¹⁴A. S. Darling, *Platinum Met. Rev.* **7**, 96 (1963), available at <https://www.technology.matthey.com/article/7/3/96-104/>.

¹⁵See <https://ec.europa.eu/growth/sectors/raw-materials/specific-interest/critical> for information about critical raw materials.

¹⁶T. Kojima, *J. Phys.: Condens. Matter* **26**, 064207 (2014).

¹⁷E. Poirier, F. E. Pinkerton, R. Kubic, R. K. Mishra, N. Bordeaux, A. Mubarak, L. H. Lewis, J. I. Goldstein, R. Skomski, and K. Barnak, *J. Appl. Phys.* **117**, 17E318 (2015).

¹⁸H. Kono, *J. Phys. Soc. Jpn.* **13**, 1444 (1958).

¹⁹A. J. J. Koch, P. Hokkeling, M. G. Van der Steeg, and K. J. de Vos, *J. Appl. Phys.* **31**, S75 (1960).

²⁰J. H. Park, Y. K. Hong, S. Bae, J. J. Lee, J. Jalli, G. S. Abo, N. Neveu, S. G. Kim, C. J. Choi, and J. G. Lee, *J. Appl. Phys.* **107**, 09A731 (2010).

²¹J. M. D. Coey, *J. Phys.: Condens. Matter* **26**, 064211 (2014).

²²T. Ohtani, N. Kato, S. Kojima, K. Kojima, and Y. Sakamoto, *IEEE Trans. Magn.* **13**, 1328 (1977).

²³*Modern Methods of Crystal Structure Predictions*, edited by A. R. Oganov (Wiley-VCH Verlag & Co. KGaA, 2011), p. 228.

²⁴S. Curtarolo, W. Setyawan, S. Wang, J. Xue, K. Yang, R. H. Taylor, L. J. Nelson, G. L. W. Hart, S. Sanvito, M. Buongiorno-Nardelli, N. Mingo, and O. Levy, *Comput. Mater. Sci.* **58**, 227 (2012).